JOURNAL OF GEOPHYSICAL RESEARCH, VOL. 96, NO. B12, PAGES 19,825–19,842, NOVEMBER 10, 1991

Mapping of Low *P* Wave Velocity Structures in the Subducting Plate of the Central New Hebrides, Southwest Pacific

R. PREVOT[1,2], S. W. ROECKER[3], B. L. ISACKS[1], AND J. L. CHATELAIN[2]

Arrival times of compressional (*P*) and shear (*S*) waves generated by earthquakes located in the New Hebrides subduction zone and recorded by local and regional arrays of seismographs are used to determine large-scale one- and three-dimensional elastic wave velocity structures of the subduction zone between 15° and 20°S and from the surface to about 250 km depth. The results obtained from inverting the locally and regionally recorded arrival times individually corroborate each other, and they are inverted jointly in order to improve the resolution of shallow to intermediate depth structures. The results for one-dimensional structure indicate a gradual increase of velocity with depth until a 9% reversal appears between 60 and 100 km depth. The three-dimensional structure determined from the joint inversion shows that these low velocities lie within a sizable seismic gap in the descending Benioff zone. Taken with other observations such as the attenuation of high-frequency shear waves travelling across this gap and the locations of active volcanoes at the surface, we infer that the low-velocity region represents a thermal anomaly of about 750°C which alters the physical properties of the descending plate in this region. At shallower depths there is evidence of low-velocity structures included in the descending plate: one beneath north Malekula island and another between Malekula and Efate islands corresponding to the large embayment of the leading edge of the upper plate. The locations of these structures combined with previous investigations of the area lead us to infer that these low velocities are due to the subduction of small-scale features such as seamounts and accretionary wedges.

INTRODUCTION

The New Hebrides arc is part of a larger island arc system that forms the boundary between the subducting Indo-Australian plate and the overriding Pacific plate (Figure 1). Convergence between the two plates occurs here at a rate of about 11 cm/yr and in a direction approximately normal to the trench [*Dubois et al.*, 1977]. The present New Hebrides arc has been a region of active subduction for probably less than 6-8 m.y., having inherited this role when an ancestral Solomon-New Hebrides-Fiji-Tonga subduction zone was disrupted in the late Miocene [e.g., *Karig and Mammerickx*, 1972; *Hamburger and Isacks*, 1987]. The arc appears simple on a regional scale, being nearly linear along its 1200 km length from the Santa Cruz islands to the Hunter fracture zone. The upper plate is morphologically complex, however, with the most striking structural anomalies occurring in the central part of the arc between 14°and 17°S. In this area, the normal trench, island arc and back arc rift systems that occur elsewhere along the upper plate are replaced by the western island blocks of Santo and Malekula, the central Aoba basin and the horst-like structure beneath the eastern islands of Maewo and Pentecost, respectively. Directly to the west of these structures, on the subducting plate, is a broad, east-west oriented topographic high known as the D'Entrecasteaux Fracture Zone (DFZ) [*Mammerickx et al.*, 1973; *Daniel et al.*, 1977; *Maillet et al.*, 1982; *Collot and Fisher*, 1991; *Fisher et al.*, 1991].

Hypotheses concerning the history of the structures in the central New Hebrides arc are controversial. One scenario proposes an episode of rifting on the late Miocene that resulted in the migration of Santo and Malekula to the west with the creation of the Aoba basin [e.g., *Karig and Mammerickx*, 1972]. This primary stage of extension was later replaced by one of compression, resulting in the uplift of the islands of Maewo and Pentecost along steep, reactivated normal faults that once bordered a graben [*Mallick and Neef*, 1974; *Carney and Macfarlane*, 1978; *Isacks et al.*, 1981]. The emergence of the limestone reef caps on the islands of Efate, Erromango, and Aniwa to the south and on the Torres islands to the north may similarly be the result of recent uplift [*Mitchell and Warden*, 1971; *Bloom et al.*, 1978; *Bevis and Isacks*, 1981]. While feasible in many respects, however, this scenario is not unique, and other mechanisms attributing most of the morphology strictly to the interactions with the DFZ have been proposed [*Chung and Kanamori*, 1978a, b].

Much of the current deformation in the central part of the upper plate does appear to be strongly influenced by the DFZ, which intersects the trench in this area. Subduction of the DFZ is probably responsible for the Quaternary uplift and tilting of Santo and Malekula [*Taylor et al.*, 1980; *Gilpin*, 1982], and the location of two ridges that bound the subducted DFZ may be reflected in major east-west tilt discontinuities located in southern Santo and northern Malekula [*Isacks et al.*, 1981]. Moreover, the volcanoes on the islands of Ambrym, Aoba and western Epi are arranged in linear trends that radiate away from the intersection of the southern boundary of the DFZ with the trench [*Roca*, 1978]. Finally, the reactivated normal faults on Santo and on either side of Maewo and Pentecost are probably due to convergence with the DFZ [*Mallick and Greenbaum*, 1977; *Isacks et al.*, 1981].

[1] Institute for the Study of the Continents, Cornell University, Ithaca, New York.

[2] Institut Français de Recherche Scientifique pour le Développement en Coopération, ORSTOM, Noumea, New Caledonia.

[3] Department of Earth and Environmental Sciences, Rensselaer Polytechnic Institute, Troy, New York .

Copyright 1991 by the American Geophysical Union.

Paper number 91JB01837.
0148-0227/91/91JB-01837$05.00

O.R.S.T.O.M. Fonds Documentaire

O.R.S.T.O.M. Fonds Documentaire
N° : 35500 Ex 1
Cote : B p80 M

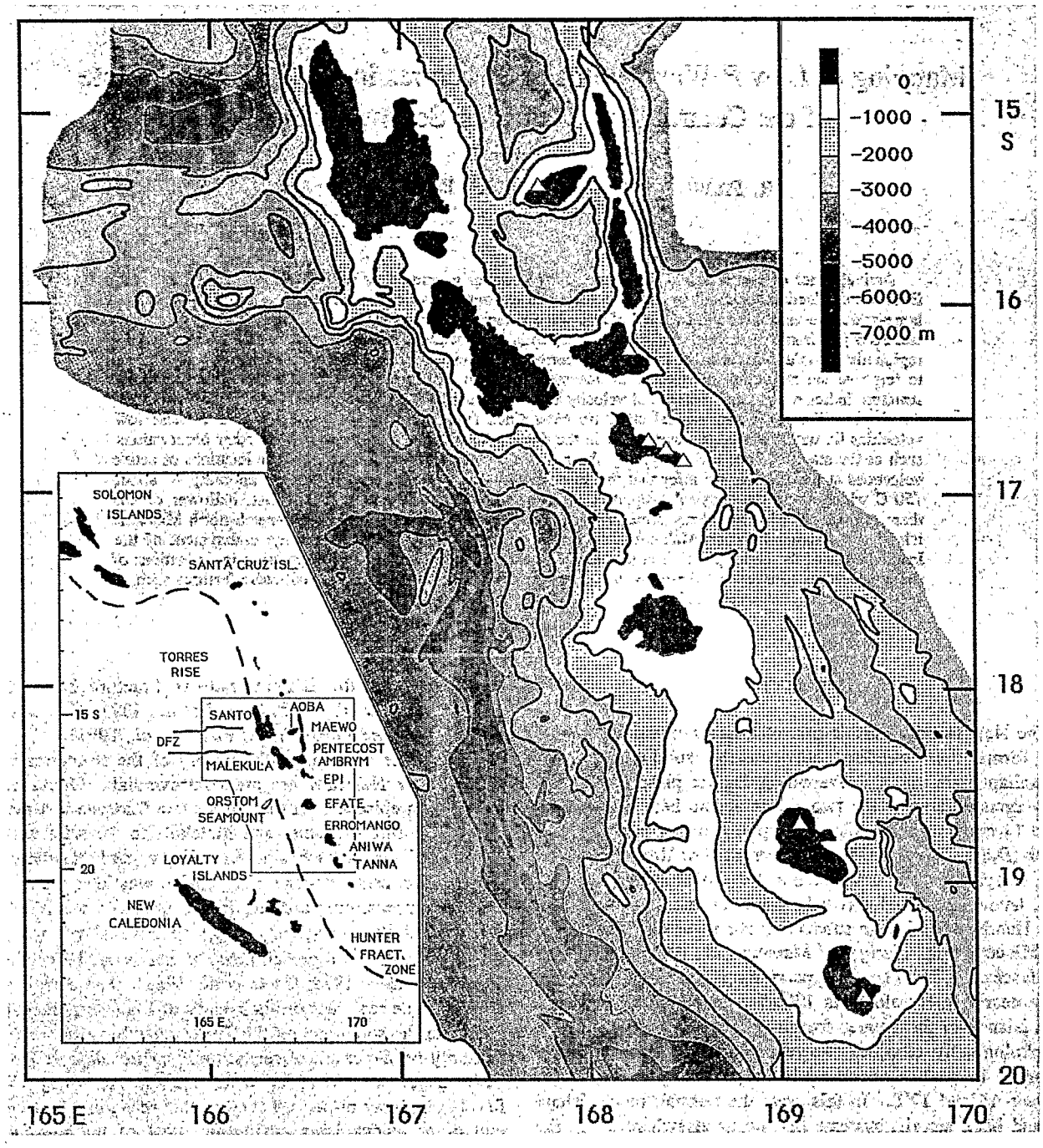

Fig. 1. Bathymetric map of the central New Hebrides Island arc adapted from *Monzier et al.* [1984] and from *Mammerickx et al.* [1973]. The open triangles denote Quaternary volcanoes and the dashed line in the inset map denotes the New Hebrides trench.

In contrast to its active role near the surface, the DFZ appears to have little influence on the geometry of the deeper subduction zone. Cross sections of teleseismically recorded earthquakes [*Pascal et al.*, 1978; *Isacks and Barazangi*, 1977] reveal a consistently simple pattern all along the arc, with the seismicity confined to a narrow, steeply dipping (70°) zone. Fault plane solutions from deep earthquakes directly beneath the DFZ have been used to infer the existence of the subducted DFZ to depths of 100-250 km [*Pascal et al.*, 1978; *Chung and Kanamori*, 1978b]. At the same time, because the DFZ is aligned obliquely to the direction of convergence at the surface, geometric arguments [*Marthelot et al.*, 1985] imply that its position at depth must be south of its position at the surface. This reasoning suggests a correlation between the subducted DFZ and a sizeable gap of the seismicity along the arc. Moreover, elastic waves travelling through this seismic gap appear to be much more attenuated than those passing outside of the gap [*Marthelot et al.*, 1985], suggesting an anomalous structure or a discontinuity in the slab in this region.

In addition to the DFZ, there are several other topographic highs on the subducting plate near the trench. The Torres rise to the north and the Loyalty islands and New Caledonia to the south are major structures that will encounter the trench within the next few million years. The Loyalty basin is also littered with smaller scale structures, at least one of which, the ORSTOM seamount, is presently at the plate boundary. It

TABLE 1. Stations of the Local Seismic Network

Name	Weight	Latitude °S	Longitude °E	Elevation m	Operated year	Island	Seismometer	
HOG	1	15 08.10	167 08.30	105	1980-1987	Santo	4.5 Hz	Z
VAN	1	15 20.60	167 00.10	488	1979-1987	Santo	4.5 Hz	Z, H(1980)
SSO	1	15 39.30	166 48.60	238	1979-1987	Santo	4.5 Hz	Z, H(1981-1987)
MAL	1	15 39.70	167 06.50	327	1979-1987	Malo	4.5 Hz	Z
AOB	1	15 26.10	167 43.15	488	1980-1987	Aoba	4.5 Hz	Z
MWO	1	14 55.67	168 03.20	165	1986-1987	Maewo	4.5 Hz	Z
PNT	1	15 46.75	168 09.25	40	1986-1987	Pentecost	4.5 Hz	Z
AMK	1	16 05.10	167 12.40	610	1980-1987	Malekula	4.5 Hz	Z, H(1986-1987)
SMT	1	16 11.25	167 30.75	160	1978-1987	Malekula	4.5 Hz	Z
LMP	1	16 28.32	167 49.18	138	1978-1988	Malekula	4.5 Hz	Z
SWB	1	16 30.52	167 25.22	305	1978-1988	Malekula	4.5 Hz	Z, H(1978-1988)
AMB	1	16 14.75	167 55.40	294	1978-1988	Ambrym	4.5 Hz	Z, H(1987-1988)
EME	1	17 05.45	168 21.07	527	1978-1988	Emae	4.5 Hz	Z, H(1987-1988)
EPI	1	16 41.70	168 06.97	188	1978-1988	Epi	4.5 Hz	Z
NGA	1	17 27.12	168 20.42	593	1978-1988	Nguna	4.5 Hz	Z, H(1987-1988)
MBV	1	17 39.52	168 18.63	471	1978-1988	Efate	4.5 Hz	Z, H(1987-1988)
RTV	1	17 47.55	168 25.48	99	1978-1988	Efate	4.5 Hz	Z, H(1987-1988)
DVP	1	17 43.52	168 11.22	77	1978-1988	Efate	4.5 Hz	Z, H(1979-1988)
ERO	1	18 51.80	169 01.35	632	1979-1987	Erromango	4.5 Hz	Z, H(1980)
TAN	1	19 29.93	169 17.17	499	1982-1984	Tanna	4.5 Hz	Z
INH	1	19 32.83	169 16.38	83	1978-1979	Tanna	4.5 Hz	Z
ANI	1	19 14.20	169 35.50	22	1979-1984	Aniwa	4.5 Hz	Z, H(1980)
LUG	0.3	15 31.07	167 07.80	144	1978-1980	Santo	1 Hz	Z, N, E
PVC	0.3	17 44.40	168 18.72	77	1978-1988	Efate	1 Hz	Z, N, E
NOU	0.3	22 18.60	166 27.03	105	1978-1987	New Caledonia	1 Hz	Z, N, E
KOU	0.3	20 33.72	164 16.88	16	1978-1986	New Caledonia	1 Hz	Z, N, E
DZM	0.3	22 04.27	166 26.67	1200	1985-1988	New Caledonia	1 Hz	Z, N, E
OBS1	1	17 58.00	167 43.50	-3550	1978	West Efate	4.5 Hz	Z
OBS3	1	17 28.10	167 40.70	-3500	1978	West Efate	4.5 Hz	Z
OBS4	1	16 51.00	167 25.00	-2610	1978	West Efate	4.5 Hz	Z
OBS5	1	16 48.67	167 44.60	-1890	1978	West Efate	4.5 Hz	Z
OBS6	1	17 19.35	167 53.82	-3440	1978	West Efate	4.5 Hz	Z
OBS7	1	17 36.00	167 56.50	-1390	1978	West Efate	4.5 Hz	Z
OBS8	1	17 52.00	167 57.50	-2160	1978	West Efate	4.5 Hz	Z
OBS9	1	14 40.00	167 35.00	-3320	1985	North Maewo	4.5 Hz	Z

Columns are the station name, relative weight, latitude, longitude, elevation, years of activity between 1978 and 1988, island name where the station is located. Last column gives a short description of the station seismometer(s): natural frequency (4.5 or 1 Hz) and components (Z,N,E). H denotes a station equiped with an horizontal component followed by its period of activity.

seems reasonable, therefore, to surmise that the subduction of features similar to the DFZ has happened in this area before.

Because the physical properties of structures such as the DFZ are different from those of normal oceanic lithosphere, the disposition of these structures at depth may be reflected in the elastic wave velocity structures of the region. In this paper we discuss the results of a study of the one- and three-dimensional compressional (P) wave velocity structure of the central New Hebrides subduction zone. This study focuses on the large-scale structure of the arc from 15° to 20°S and from the surface to about 250 km. The structures deduced are used to refine the locations of earthquakes hypocenters, which can then be used along with the velocity structures in making inferences concerning the tectonics of the region.

DATA

Two different sets of data are used in this study. One set includes arrival times of P and S waves of local events recorded between 1978 and 1988 by a local telemetered seismic network. The second set is taken from the catalog of arrival times reported to the International Seismological Centre (ISC) by all stations operating in the southwest Pacific between 1964 and 1983. There is little overlap between these two data sets because of the procedure used to select the events. Only 14 events overlap in our zone of study, and their differences in location increase from 10 km in any direction for shallow events located near the center of the network (17°S) to 30 km for deep events or events located far to the north or far to the south. Specifically, locally recorded events had to be small enough that S waves could be identified on some subset of stations, whereas regionally recorded events had to be large enough to be reported by at least 30 stations. These requirements tend to be mutually exclusive.

Local Data

Most of the arrival times of the local data set were recorded by a seismic network composed of 27 land-based stations (Table 1 and Figure 2). Twenty-two of these stations compose

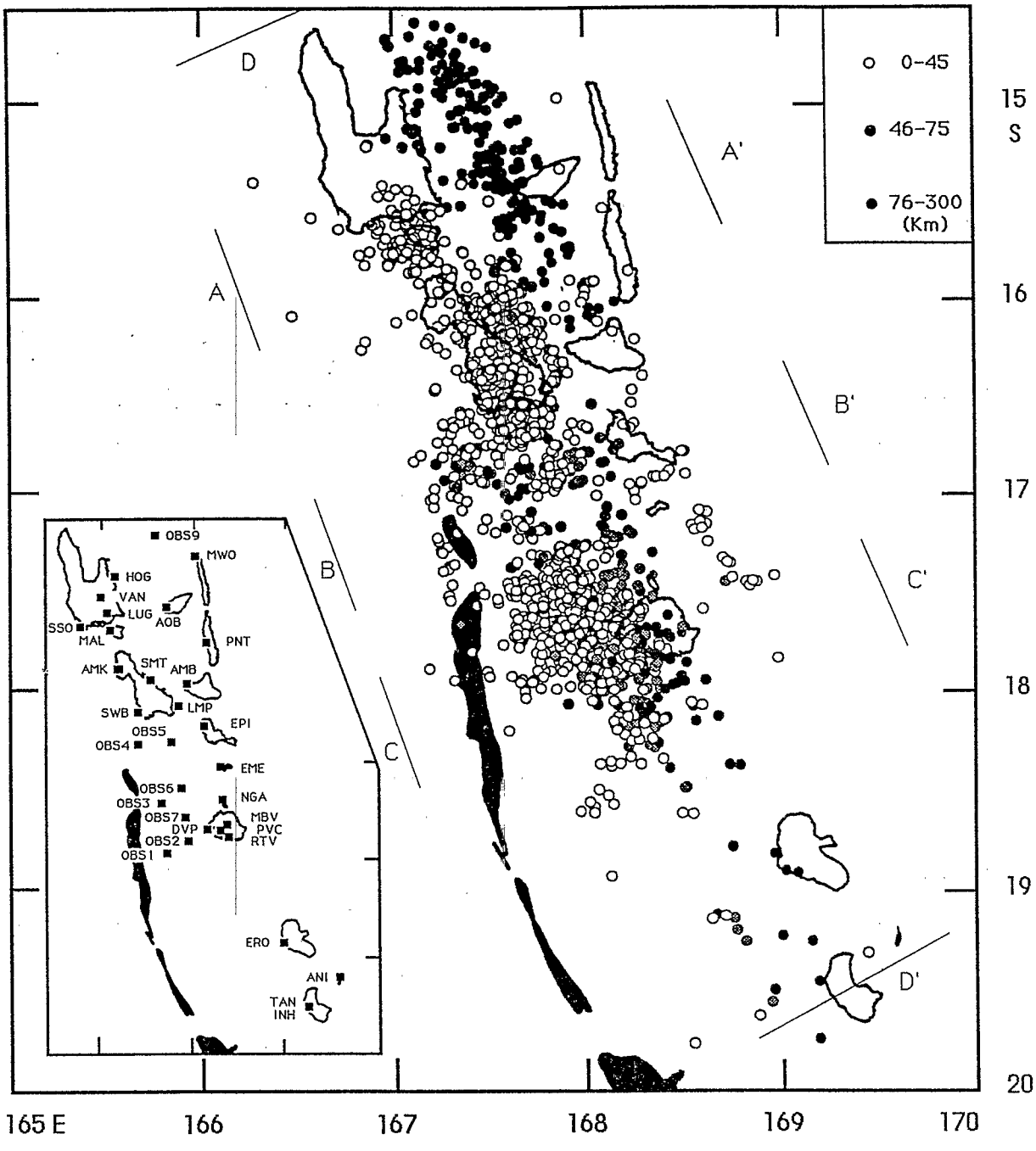

Fig. 2. Map view of the events located by the local seismic network. Seismic stations of the local telemetered network are shown in the inset map . Sections A-A', B-B', C-C', and D-D' are shown in Figures 9, 10, 11, and 12.

the telemetered array installed and operated since 1978 by the Institut Français de Recherche Scientifique pour le Développement en Coopération (ORSTOM) and by Cornell University. The five remaining land-based stations (Luganville (LUG), Port Vila (PVC), Koumac (KOU), Noumea (NOU), and Dzumac (DZM)) are part of the worldwide seismological network operated by ORSTOM.

In addition to these land based stations, an array of eight ocean bottom seismographs (OBS) was operated west of Efate during September 1978, in collaboration with members of the University of Texas. In April and May 1985, one OBS (OBS 9) and two land stations (MWO and PNT) were operated. These two land stations were reopened in 1986 as part of the telemetered seismic network (Table 1 and Figure 2)

All of the arrival times were read by ORSTOM technicians with the exception of those recorded during the September 1978 survey, which were read by members of the University of Texas and Cornell University. The *P* arrival times reported from the telemetered and OBS networks are estimated to have a precision of 0.05 s, while those from stations LUG, NOU, DZM, KOU, and PVC have an estimated precision of 0.1 s. This difference is due largely to a difference in reading

technique (using a digitizing table rather than a ruler). The precision of S wave readings is generally considered to be 3-4 times worse than that of the corresponding P wave, with higher precision assigned to those arrivals recorded by seismometers with horizontal components.

Approximately 25,500 local earthquakes have been located using data from the local network between 1978 and 1988. This abundance of earthquakes allowed us to be conservative in selecting data to use in the velocity inversions. As a first filter, we kept only those events that ostensibly were well recorded (more than 10 total arrival times with a minimum of three S waves). A preliminary data set of some 13,892 earthquakes was thus compiled. These events were relocated in a one-dimensional structure (Table 2) derived from a compilation of results of various investigators [*Dubois et al.*, 1973; *Kaila and Krishna*, 1978; *Ibrahim et al.*, 1980; *Coudert et al.*, 1981, 1984]. Various statistical quantities such as the root-mean-square (RMS) residual, the standard deviation of the hypocenter coordinates, the convergence properties of the iterated location, and the condition number of the matrix of location partial derivatives were used to assess the quality of the locations. Moreover, to insure that the locations of events kept for inversion were not overly dependant upon the velocity structure, selected events were relocated in a perturbed (5-7% difference) one-dimensional structure and compared with the original estimate. At the beginning of the analysis, those events with locations that differed by more than 5 km in any direction were eliminated. A starting set of 2027 events, composed of 17,257 P and 13,721 S arrivals, was thus compiled. After a reliable one-dimensional structure was determined from this set of data, the relocation requirement was relaxed to 10 km for events in sparsely sampled areas in order to improve the resolution of complicated near-surface structure. A resulting 4181 events, composed of 35,816 P and 29,014 S arrivals, was then used to determine three-dimensional structures.

Observations were given weights according to their expected uncertainties, and data errors are presumed to be uncorrelated. In general, S phases were given one tenth of the weight of corresponding P arrivals, and arrivals at stations KOU, NOU, DZM, PVC, and LUG were assigned one-third the weight of those at other stations. Residuals greater than 4 s in magnitude were considered to be outliers and given zero weights.

ISC Data

Arrival times from 1000 events occurring in the New Hebrides from 14° to 20°S reported by the ISC between 1964 and 1983 were taken from the catalog (Figure 3). We selected the 38 seismic stations within a distance of 40° to our zone of investigation and, as a first cut on location quality, required that each of the selected events be reported by at least 30 stations in the ISC catalog. As a second cut, P arrivals with residuals greater than 4 s were rejected. Finally, qualified P arrivals were assumed to have a precision of 0.2 s and were given the same weight. S arrival times from this data set were not used because few of them are reported in the ISC catalog and those that are generally are associated with large residuals. The velocity model used to locate these events is the same as that used for the locally recorded data but extended in depth according to the PREM model of *Dziewonski and Anderson* [1981]. The qualities of the locations of these events were assessed using the same procedure as that used for the local data. As a result, a final set of 617 events was selected for determining an independent estimate of one-dimensional structure. In determining the three-dimensional structure, the initial set of events was augmented to 1263 by extending the zone under consideration from 13° to 21°S . After deleting the less well constrained locations, a final set of 787 events was selected for use in determining three-dimensional structures.

METHOD

We use arrival times of P and S waves recorded by local and regional seismic networks to simultaneously determine hypocenters and seismic velocities. The principal technique, based on the method of *Aki and Lee* [1976], is similar to that used by *Roecker* [1982], *Roecker et al.* [1987], and *Abers and Roecker* [1991]. A full explanation of the method can be found

Table 2. One-Dimensional P Wave and S Wave Velocity Structure

Depth to Top of Layer, km	P Velocity, km/s				S Velocity, km/s			
	Starting Model	Final Model			Starting Model	Final Model		
		Local Data	ISC Data	Local + ISC data		Local Data	Local + ISC Data	V_P/V_S
-2	5.20	6.18(0.08)	4.46(0.28)	6.60(0.06)	2.92	3.23(0.04)	3.53(0.03)	1.87
15	7.20	6.91(0.06)	7.39(0.45)	7.21(0.06)	4.04	3.86(0.04)	4.03(0.04)	1.79
30	8.06	7.61(0.05)	7.61(0.06)	7.91(0.04)	4.53	4.31(0.04)	4.43(0.04)	1.79
45	8.06	8.15(0.04)	7.95(0.04)	8.05(0.13)	4.53	4.59(0.04)	4.55(0.05)	1.77
60	8.06	7.87(0.30)	7.94(0.01)	7.94(0.04)	4.53	4.34(0.18)	4.44(0.17)	1.79
75	8.06	7.38(0.45)	7.78(0.10)	7.72(0.19)	4.53	4.02(0.16)	4.13(0.16)	1.87
100	8.13	8.14(0.10)	8.05(0.02)	8.08(0.04)	4.57	4.58(0.07)	4.56(0.07)	1.77
170	8.19	8.19(0.57)	8.22(0.02)	8.29(0.02)	4.59	4.60(0.31)	4.59(0.28)	1.81
270	8.76		8.67(0.01)	8.61(0.02)				
370	9.19		8.42(0.01)	8.40(0.06)				
470	9.96		10.21(0.01)	10.22(0.01)				
670	10.75		10.91(0.01)	10.97(0.01)				

Values in brackets are standard deviations.

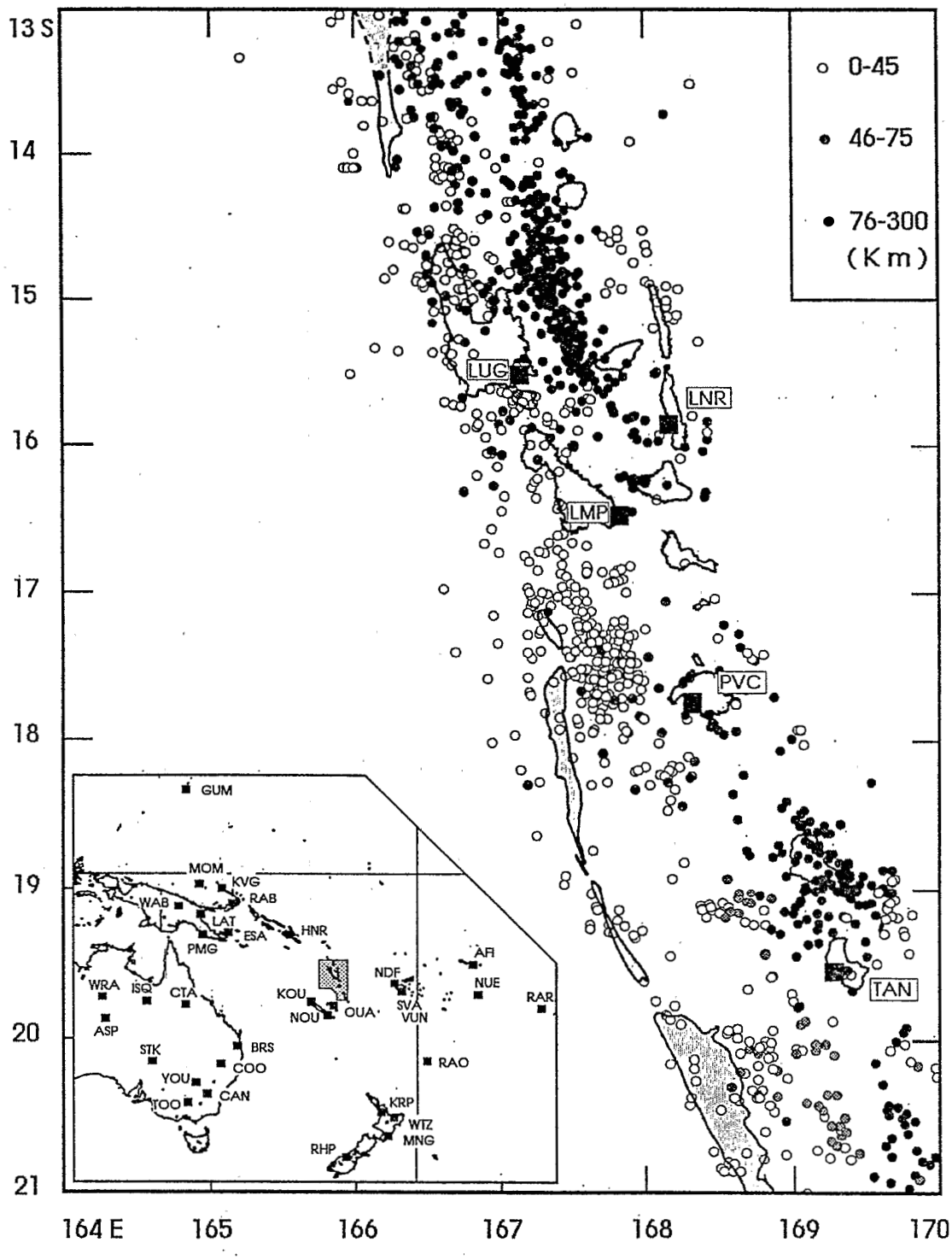

Fig. 3. Map view of the teleseismically recorded events taken from the ISC catalog between 1964 and 1983. The regional array of stations is shown in the box.

in those papers; the description below outlines the technique and emphasizes the differences between previous approaches and the ones used in this study.

We parameterize the Earth as a set of constant velocity blocks of arbitrary dimension. P and S wave velocities are specified and solved for as independent parameters. Rays through the structure are traced using an approximate ray tracer similar to that used by *Thurber and Ellsworth* [1980]. Because of the size of the region under study, we adopt the Earth-flattening transform incorporated by *Abers and Roecker* [1991] to correct for curvature. We also make use of the reparameterization technique [*Abers and Roecker*, 1991] to allow us to introduce irregular boundaries into the structure and to combine parameters that are poorly resolved. The inversions follow an iterative nonlinear formulation similar to that described by *Tarantola and Valette* [1982]. The a priori

model covariance matrix is assumed to be diagonal (no coupling between blocks) and the a priori model variances for velocities are usually assumed to be about 7%.

The inversion was iterated until changes in velocities became small (<1-2%) and variance reduction became insignificant; generally two or three iterations were sufficient. We incorporate the philosophy of progressive inversion [*Roecker*, 1982] and the technique of parameter separation [*Pavlis and Booker*, 1980] in adjusting the combined hypocenter/velocity inverse problem. Generally speaking, this means that we try to explain as much residual as possible by relocating earthquakes or calculating station corrections before perturbing the structure but still formally decouple the hypocenter parameters from the velocity parameters when solving for structural perturbations.

In analyzing the arrivals recorded at stations at regional distances, we presume that the parts of the ray paths to a given station outside of the region of interest pass though approximately the same structure, or, equivalently, that the perturbation to travel time caused by this external structure is the same for all rays arriving at a given station. Given the large distance between the earthquakes and the stations compared to the dimension of the zone of investigation (Figure 3), this seems to be a reasonable assumption. We can therefore correct for structure outside of the region of interest by calculating a "station correction" from the average residual at the station. The residual remaining after the station correction is applied is taken to be due to anomalous structure within the region of interest.

The principal reasons for including the regionally recorded data were (1) to provide results from a somewhat independent data set in order to assess the reliability of the structure deduced from analysis of the local data alone and (2) to improve the resolution of various structures by performing a joint inversion of both types of data. Below we will review the results of inverting these two types of data independently and jointly.

RESULTS

Generally speaking, the regions over which we can hope to determine the structure beneath the New Hebrides are those in which many seismic ray paths cross each other. An examination of the source-receiver configurations (Figures 1, 2, and 3) reveals that these regions are the leading edge of the upper plate and the descending Wadati-Benioff zone. Outside of these volumes, ray paths are sparse or nearly parallel, and thus we expect that the upper mantle surrounding the seismic zone will be poorly constrained.

Following the philosophy of progressive inversion [*Roecker*, 1982], we began our analysis by first determining simple (starting with one-dimensional) structures and moving on to more complicated structures as the data required. For comparative purposes we analyzed each of our two data sets separately and then jointly to understand better the effects of these types of data on the structures determined.

One-Dimensional Structures

Local data. In determining a one-dimensional velocity structure we take as our a priori model a hybrid structure determined by compiling results of previous investigators (Table 2) [*Dubois*, 1969; *Kaila and Krishna*, 1978; *Ibrahim et al.*, 1980; *Coudert et al.*, 1981; 1984]. This is the same

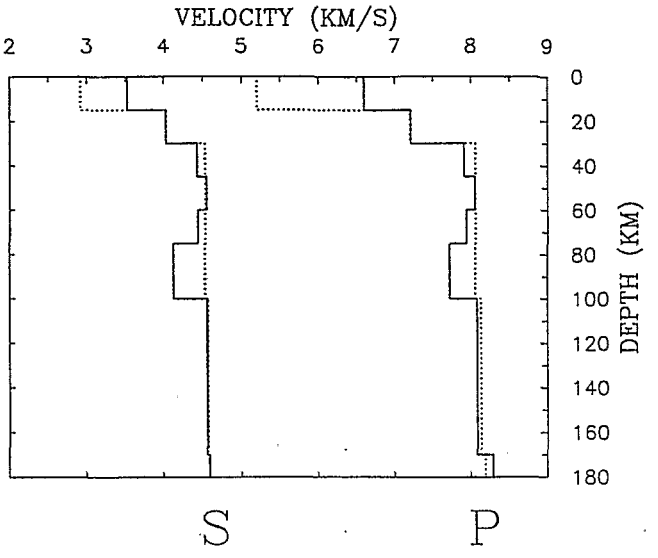

Fig. 4. One-dimensional *P* and *S* velocity structure determined from a combination of local and ISC data sets. The starting model is indicated by the dashed line.

structure used to select the data set of 2027 events from the original set of 13,892. *S* wave velocities are initially set by using a V_P/V_S ratio of 1.78, which represents an average deduced from a number of Wadati plots (see discussion by *Roecker et al.* [1988]). Station corrections were calculated as an intermediate step following the relocation of events, but a comparison of results determined with and without station corrections revealed that the deduced structures are not strongly dependent upon them. Specifically, station corrections decrease the original variance from 0.15 s^2 to 0.10 s^2 but the final residual variance is the same (0.05 s^2) in both cases. Much of the station corrections appear to be absorbed during the relocation. Generally, all significant reduction in variance was obtained after two iterations.

In the best fitting one-dimensional structure (Table 2), we see that both *P* and *S* velocities gradually increase with depth from the surface to 60 km depth. Below 60 km a reversal appears, reaching a dramatic (9%) low between 75 and 100 km. Normal mantle velocities appear again beneath 100 km. We note that the velocities above 60 km depth and between 100 and 170 km depth appear to be well resolved and the associated standard errors are small (<0.1 km/s), whereas structure in the low-velocity region is less well constrained (>0.3 km/s). This is largely because most of the ray paths traversing the low-velocity layer are refracted rays from the predominantly shallow sources, and therefore many of these paths are nearly parallel within the layer. Structure beneath 170 km depth is not well constrained because of the poor sampling at this depth. As a result of this inversion, the variance of the local data set was reduced from 0.1 to 0.05 s^2

ISC data. For purposes of comparison, and to constrain some of the less well resolved parameters determined by inverting the local data, we also determined a one-dimensional structure using the regionally recorded data. The starting velocity structure for the upper 170 km is the same as that used for local data, and is extended to 670 km depth using the velocities from the PREM model [*Dziewonski and Anderson*, 1981]. As with the local data, all significant variance

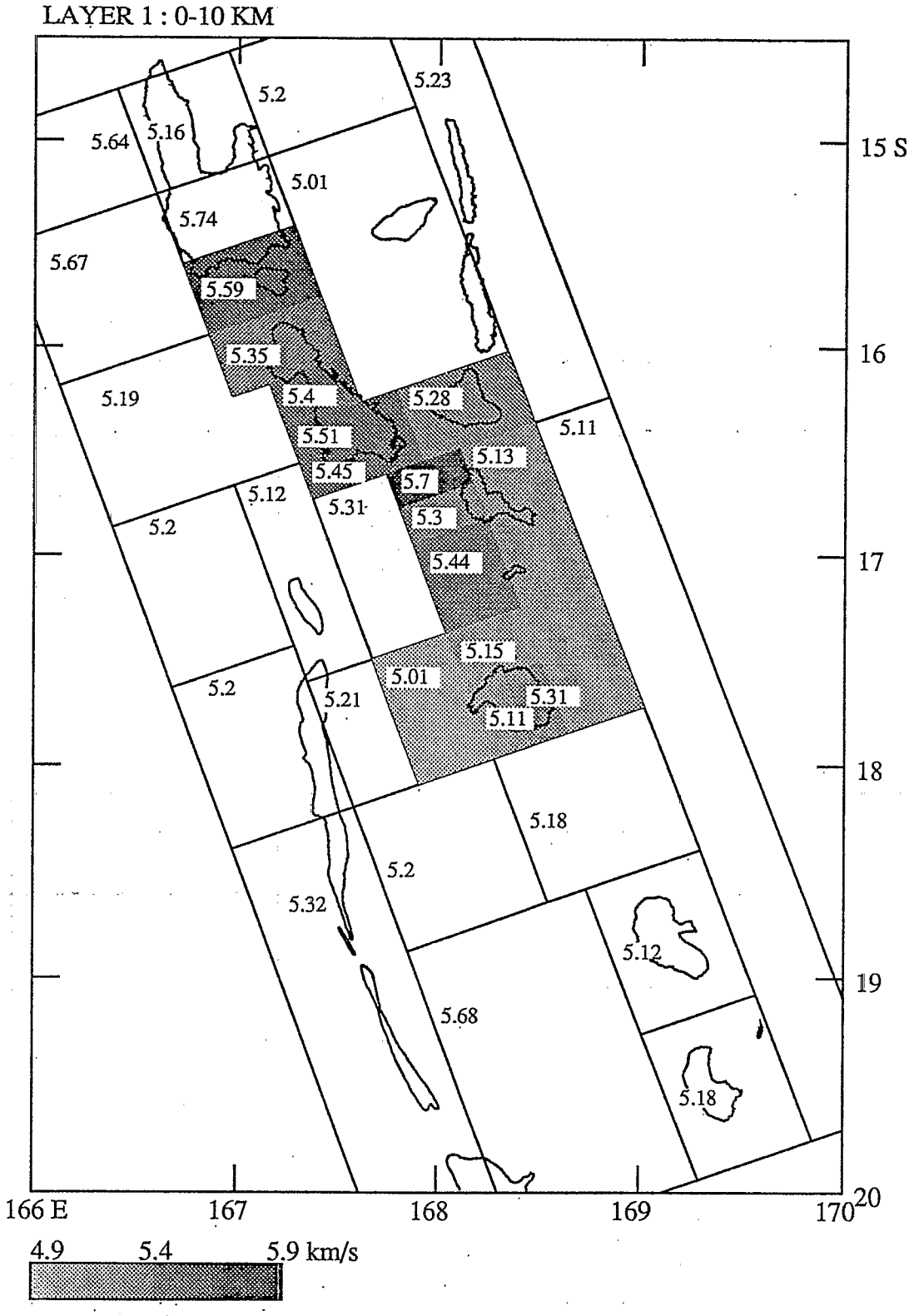

Fig. 5. Map view of *P* wave velocities in the first layer. Blocks with a resolution diagonal greater than 0.70 are shaded according to the velocity scale beneath the map.

reduction was achieved after two iterations. In applying the station corrections, the investigated volume is about the same than the one investigated by local data (see discussion in previous section).

As with the structure determined from local data alone, the most striking feature in the velocities deduced from the regional data is the low-velocity zone between 60 and 100 km depth . An additional low-velocity zone occurs between 370 and 470 km depth (Table 2), below the deepest earthquakes for which we have data. We note that the structure in the first two layers (0-30 km) are poorly resolved and have large associated errors (0.45 km/s). This lack of constraint is a consequence of

a lack of upward travelling ray paths; only five stations (LUG, LMP, LNR, PVC, and TAN) in this set are located above the seismic zone, and rays to stations outside the seismic zone do not contribute much to the inverse solution because the ray paths to these stations are almost parallel and any travel time anomaly is absorbed in the station corrections. As a result of the one-dimensional inversion, the original variance in the ISC data set of 1.47 s^2 was reduced to 0.45 s^2.

In summary, where they overlap, the one-dimensional structures deduced from the two separate data sets are consistent with one another, the most striking feature being a region of low velocity located inside the Benioff zone between 60 and 100 km depth. Combining local and ISC data sets and using as a starting velocity model the same as that used for ISC data, we can propose a final best fit one-dimensional model (Table 2 and Figure 4). Note that the low-velocity zone is preserved and smaller errors are associated with the velocities. In this case the variance decreases from 0.76 s^2 to 0.22 s^2 after two iterations. Changes in locations are about 10 km for ISC data and 5 km for local data.

At this point we are confident with the consistency of our data, and we thus seek to explain the remaining variance, and to localize the cause of the anomalously low velocities, by introducing laterally varying structures.

Three-Dimensional Structures

In determining lateral variations in velocity, a block model was designed to incorporate a priori information about structural bounds in the region, deduced either from surface geology or from patterns of seismicity. Block size was also governed by the expected ability of the data to resolve structure in a given region; in particular, heavily sampled blocks were subdivided in an attempt to recover more information on a smaller scale. Poorly sampled blocks, defined as those intercepted by less than 30 rays, were eliminated from the inversion. Generally, these blocks were located on the periphery.

As discussed in the data section, after determining one-dimensional structures with what we consider to be the best constrained locations, the number of regionally recorded events was augmented by extending the zone under consideration by 2° from 13° to 21°S. Also, to improve the resolution of the complex structure in the upper 30 km, the number of local earthquakes was increased from 2027 to 4181 by relaxing the requirement that relocated earthquakes differ by less than 5 km in different one-dimensional structures (we note that the no extra events were added to the nest of seismicity northwest of Efate).

Local and ISC data first were inverted separately. Surprisingly, the large-scale structural patterns in layers 5-7 are not significantly different. Both cross sections show a comparable low velocity zone (see appendix Figure A5 on microfiche[1]) although in some blocks resolution is low. As with the one-dimensional inversion, the main difference between the two three-dimensional solutions is in the resolution of structure: upper blocks are resolved better with local data and lower blocks with ISC data. If we were talking about photography, we might say these two pictures (Figure A5) are blurred but show the same image. A combination of these two pictures should give us a better picture in term of clearness (or resolution)

Because the regions of poor resolution for these data sets are largely complimentary, we combined them in a joint inversion and will confine further discussion to the results of this inversion. Two iterations were required before the change in variance became insignificant; the reduction in variance for the entire dataset decreased by 82% to a final value of 0.09 s^2 (in the appendix are shown parameters such as resolution, numbers of hits and errors: Figures A1, A2, A3, A4, and A6).

Shallow structure (< 30 km). In an attempt to incorporate a priori information about shallow structures into the inversion, blocks in the upper few layers were designed to fit approximately the structural units seen at the surface and the seismic boundaries determined by Chatelain et al. (1986). These blocks were subdivided into smaller blocks in places where the ray density is high enough to keep resolution greater than 0.70. The results (Figures 5-8) show that blocks with good resolution (> 0.70) are confined to a narrow strip parallel to the dominant strike of the seismic array in the area between Santo and Efate. Structure south of Efate is not well resolved above the fourth layer (< 30 km). Patterns of velocities in the first three layers are complex but may be interpreted in the framework of *Isacks et al.* [1981], who divided the upper plate into several units. Starting from the north, the first unit (Santo block) is a westward protrusion upon which are located the islands of Santo and Malekula. The Santo block does not have a clear southern boundary, but the bathymetry suggests a progressive transition between a Santo-Northern Malekula block and a Southern Malekula block (Figure 1). Velocities of the first layer (0-10 km; Figure 5) corresponding to this region decrease slightly to the south (5.59-5.40 km/s) in the northern tip of Malekula. Velocities in layers 2 and 3 (10-30 km; Figures 6 and 7) show a similar southward decrease in velocity from 7.50 to 7.18 km/s (the very high velocity of 7.86 km/s in layer 2 (10-20 km) has a large error (±0.3 km/s) associated with it). The middle of Malekula island appears to be underlain by low velocities of the order of 6.18-6.59 km/s in layer 2. Velocities within the Aoba basin, east of the Santo block, are not as well constrained as in surrounding areas but nevertheless appear to be lower than in the adjacent Santo block in the first two layers (0-20 km) and are so close in the third layer (20-30 km) that we are unable to differentiate between these two units.

The region between Southern Malekula and Efate island corresponds to the northern termination of the Southern New Hebrides trench in a large embayment in the leading edge of the upper plate and a widespread distribution of volcanic centers (Figure 1). The southern limit of this region is defined by a seismic boundary [*Chatelain et al.*, 1986] located northwest of Efate. This region is characterized by velocities in the upper three layers (0-30 km) that are significantly lower in the west than in the east. This low-velocity zone is probably related to the embayment, while the higher-velocity zone correlates with a high topographic feature upon which are located most of the islands (Figure 1).

To the south, Efate is part of a westward salient of the upper plate. The trends in velocities in this region are reversed to those in the northwest with a eastward decrease in layers 2 and 3. The first layer is characterized by generally low velocities (5.01-5.31 km/s). High velocities (> 7 km/s) in layers 2 and 3

[1] Appendix Figures A1-A6 are available with entire article on microfiche. Order from American Geophysical Union, 2000 Florida Avenue, N.W., Washington, DC 20009. Document B91-003; $2.50. Payment must accompany order.

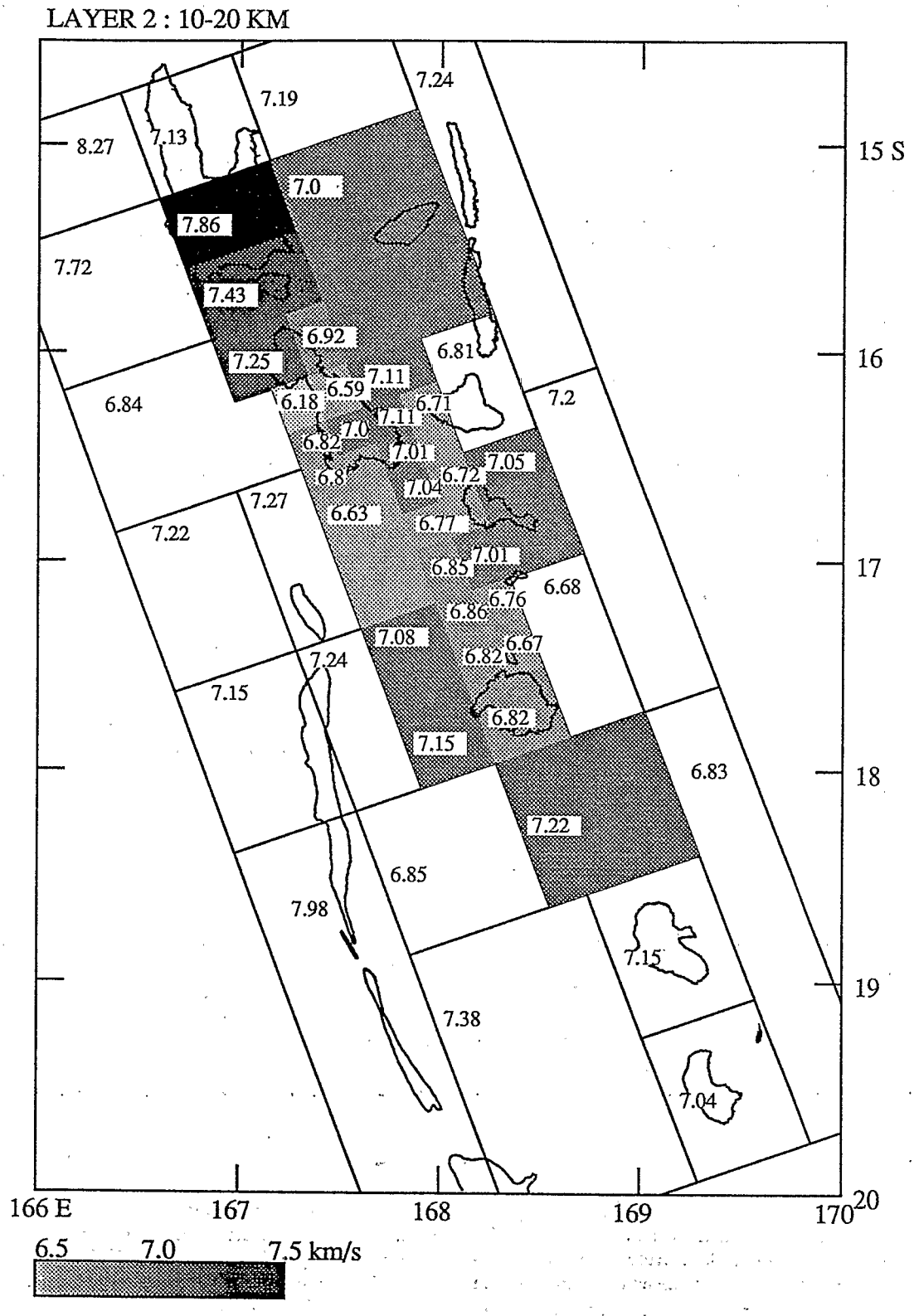

Fig. 6. Map view of *P* wave velocities in the second layer. Blocks with a resolution diagonal greater than 0.70 are shaded according to the velocity scale beneath the map.

occur in the same area as the prominent nest of seismicity northwest of Efate (Figure A3). Finally, blocks with low (6.6 km/s) velocities are located directly below Efate island within layer 3.

The shallow structure south of Efate is so poorly constrained that we cannot usefully interpret the results. The back arc region between Ambrym and Efate islands is also poorly constrained, and velocities do not show any outstanding features with the possible exception of the very low velocity (5.13 km/s) found in layer 1.

Deeper structure (>30 km). The velocity patterns in the fourth layer (30-45 km depth) are quite different from those in

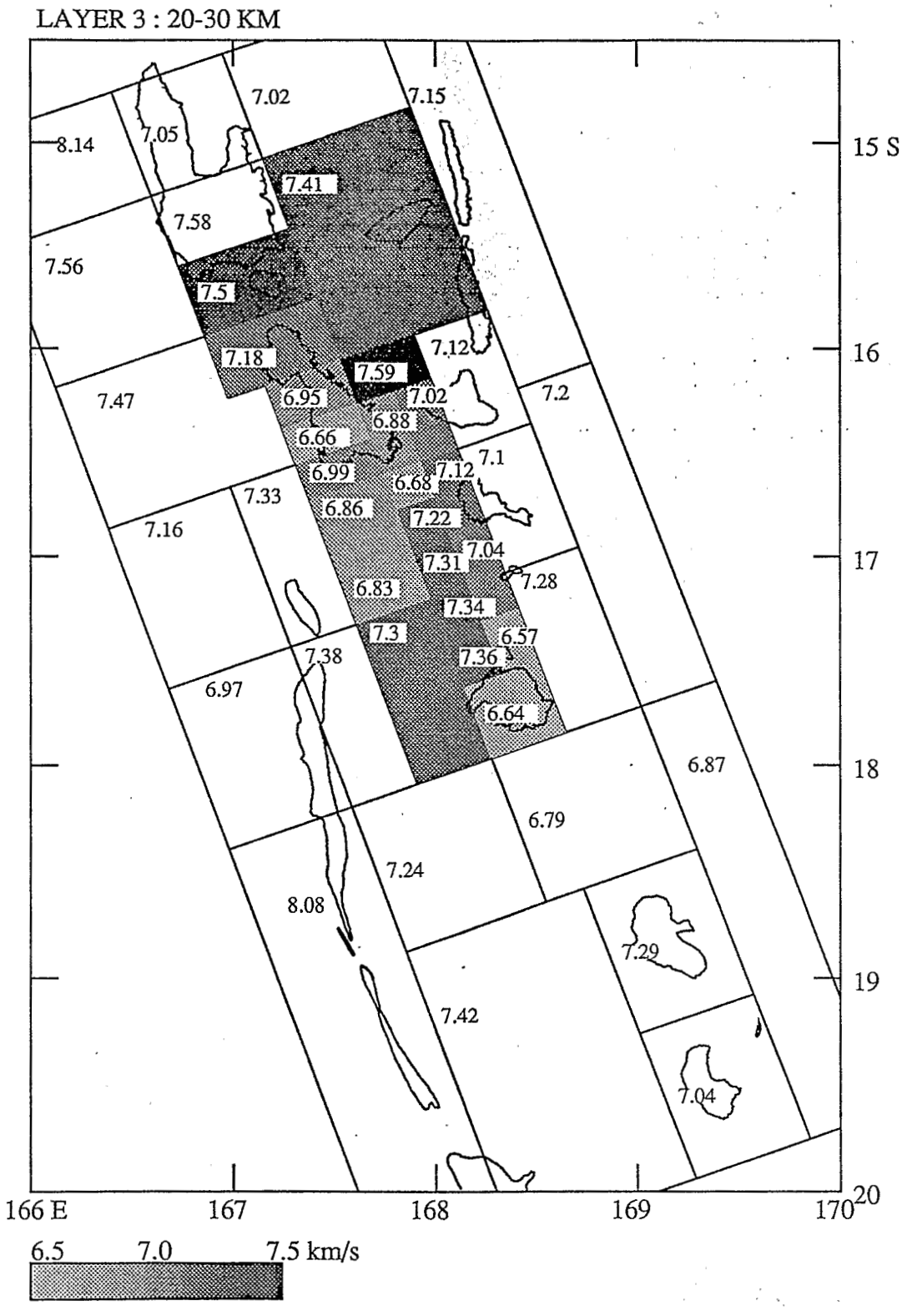

Fig. 7. Map view of *P* wave velocities in the third layer. Blocks with a resolution diagonal greater than 0.70 are shaded according to the velocity scale beneath the map

the upper three layers and therefore are not as clearly related to structure in the upper plate (Figure 8). These patterns are generally simpler than those in the upper layers, and the distribution of velocities is organized principally in an east-west direction. Higher velocities (around 8 km/s) in the west probably reflect structure within the upper mantle, while the central strip of blocks with velocities lower than 8 km/s are located near the upper edge of the downgoing slab. Of particular interest is a low in velocity (7.3 km/s) found south of Malekula island that can be related to the lows in the upper layers .

One of the main objectives of the three-dimensional

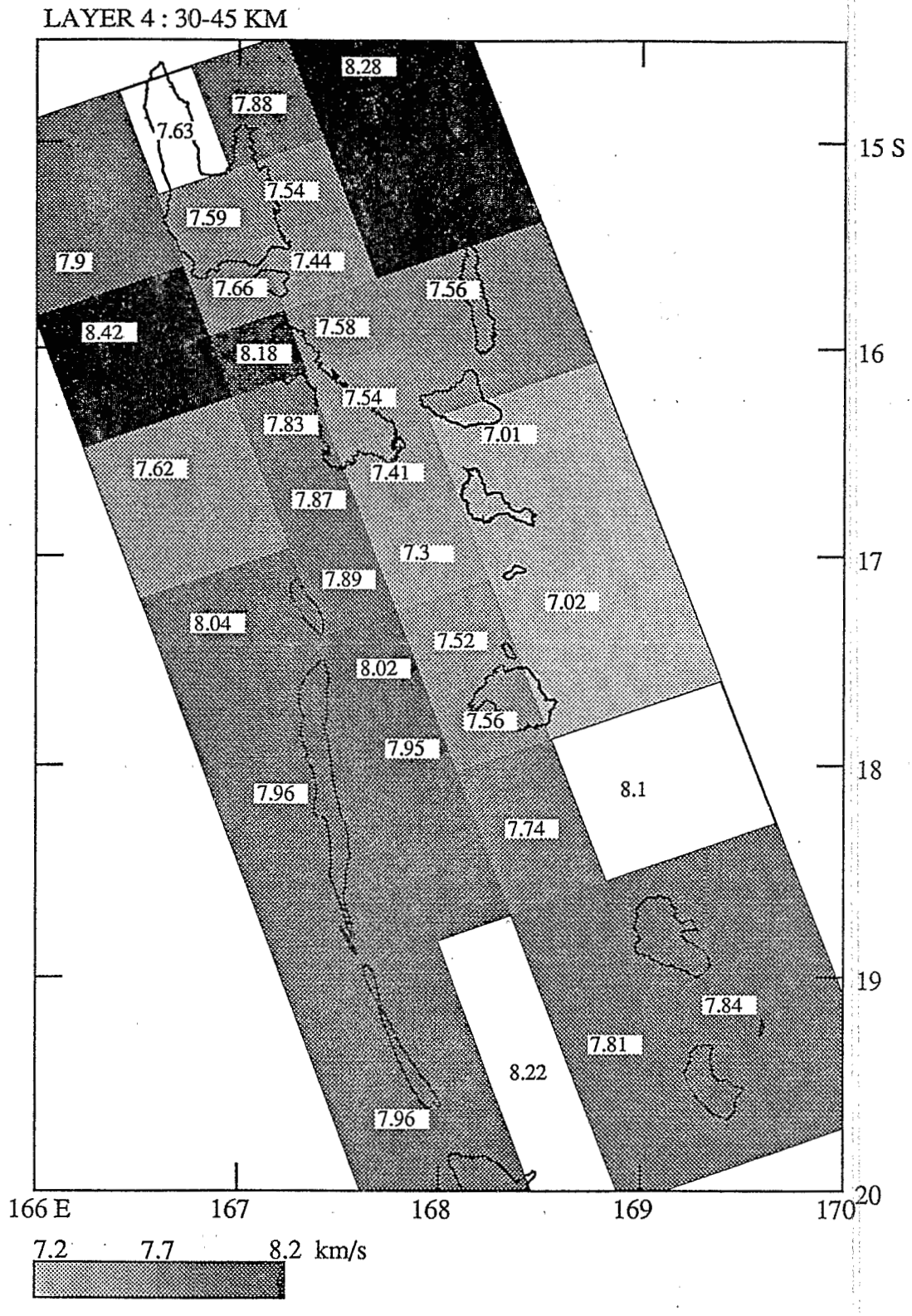

Fig. 8. Map view of *P* wave velocities in the fourth layer. Blocks with a resolution diagonal greater than 0.70 are shaded according to the velocity scale beneath the map.

inversion was to determine the cause of the dramatic reversal in velocity detected in the one-dimensional inversion. Cross sections of the results (Figure 9) show that these low velocities are confined to the region of aseismicity between about 40 and 270 km depth. All of the parameters in this low-velocity region are well resolved (>0.90) and the associated errors are reasonably small (<0.2 km/s). We note that all of these sections are confined to the region of the Wadati-Benioff zone. We report but do not interpret velocities outside the seismic zone (velocities denoted with a question mark in Figures 10-12)

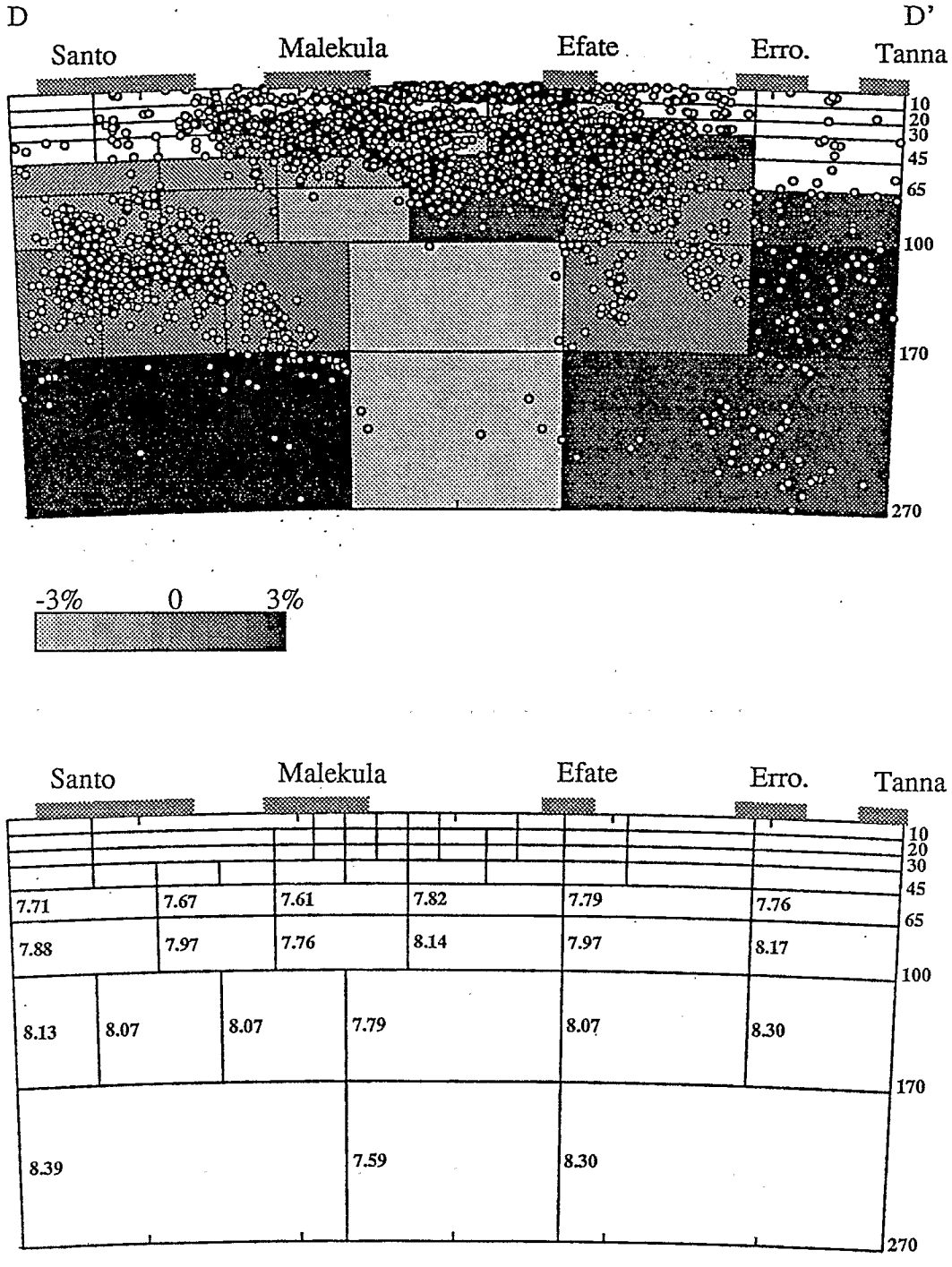

Fig. 9. Along-strike cross section D-D' of the arc as shown in Fig. 2, mapping the *P* wave velocity structure of the Wadati-Benioff zone. Blocks with a resolution greater than 0.85 are shaded according to the deviation between the block velocity and the average block velocities at the same depth. Events shown in this figure have been relocated in using this three-dimensional velocity structure. Note the overlap of the gap of intermediate seismicity by the low-velocity zone. To the bottom: *P* wave velocities in kilometers per second.

because occasional large variations from block to block could indicate that they are poorly constrained and hence unreliable. Moreover, these velocities are controlled primarily by ray paths from earthquakes in the (lower quality) ISC data set.

In order to understand better the distribution of brittle deformation within the Benioff zone, events were relocated in this new velocity structure. Relocations of the better quality events (Figures 10-12) differ from their original locations by less than 10 km (most are < 5 km) and agree with the patterns shown in previous studies [*Pascal et al.*, 1978; *Isacks et al.*, 1981]. Because we were careful to select only those hypocenters that were relatively insensitive to structure, this is not a surprising result. To examine the correlation between seismicity and velocity, we concentrate on three cross sections

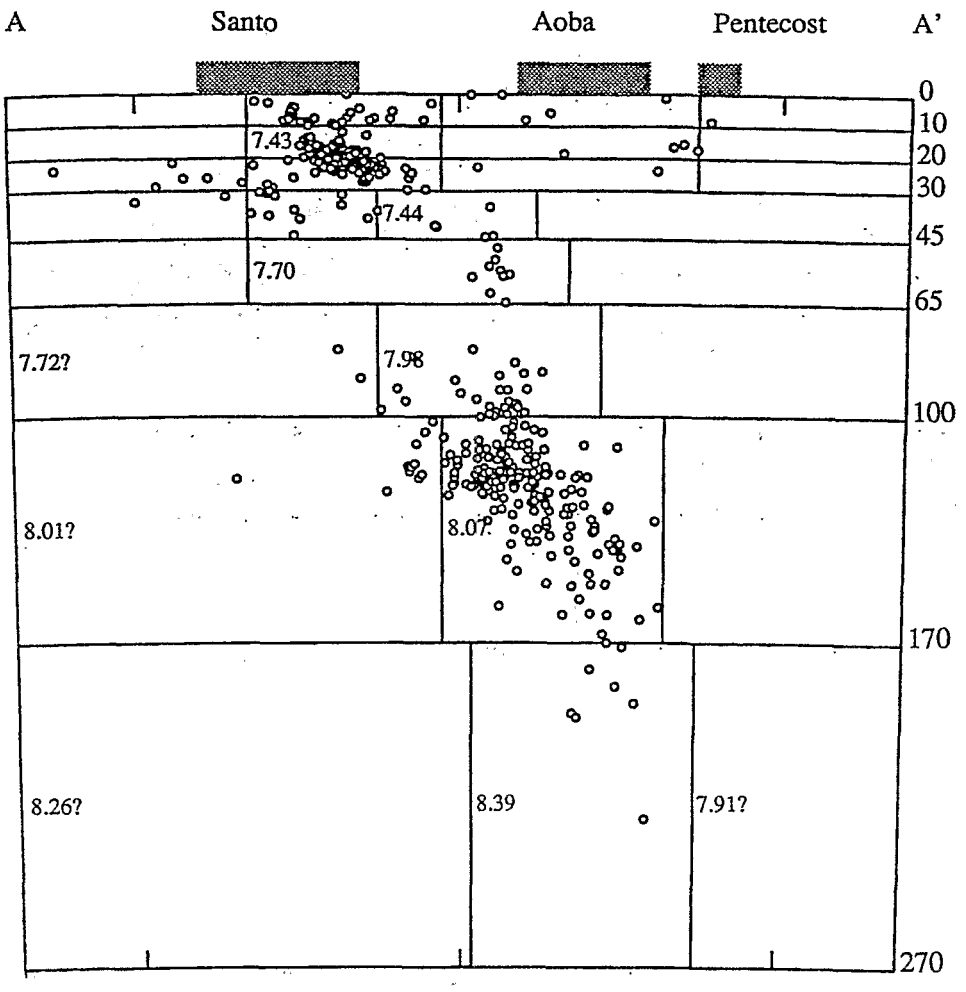

Fig. 10. Cross section along the direction A-A' as shown in Figure 2. Block velocities determined with a resolution greater than 0.85 are indicated on the figure. Velocities indicated with a question mark are considered as unreliable.

perpendicular to the trench direction that correspond to the three structural units defined by *Isacks et al.* [1981]: (1) the Santo block, which includes Santo and northern Malekula, (2) the Malekula block, which extends from the middle of Malekula to a seismic boundary northwest of Efate, and (3) the Efate block, which includes the region to the south of the seismic boundary. A comparison of cross sections through the Santo and Efate blocks (Figures 10 and 12) reveals similar steeply inclined seismic zones that are roughly 35 km thick but differences in the level and distribution of seismic activity. Most of the activity beneath the Efate block occurs at shallow depths, while that beneath the Santo block occurs at depths greater than 100 km. Velocities in both blocks increase steadily with depth: from 7.41 to 8.39 km/s in the Santo block and from 7.79 to 8.3 km/s in the Efate section. Because the change in velocity is rather uniform in these cross sections, we infer that the difference in spatial distribution of the activity is not related to large scale (hundreds of kilometers) changes in the structure of the descending plate but rather are due to local (tens of kilometers) anomalies within the slab.

The seismicity and velocities in the Malekula block (Figure 11) are quite different from those to the north and south. The seismic activity disappears below 85 km depth at the upper bound of an abnormally low-velocity structure. Also, we note in this section the presence of abnormally deep events occurring below the northern termination of the southern New Hebrides trench, some of which appear in the Santo and Efate sections away from the main Wadati-Benioff zone. The existence of these and similar events was previously reported and analyzed by *Roecker et al.* [1988].

DISCUSSION

Comparison With Other Studies

Several investigations previously have been made of the structure in and around the New Hebrides arc [e.g., *Dubois et al.*, 1973, 1977; *Ibrahim et al.*, 1980; *Goula and Pascal*, 1979; *Choudhury et al.*, 1975; *Kaila and Krishna*, 1978; *Grasso et al.*, 1983; *Coudert et al.*, 1984; *Pontoise and Tiffin*, 1986; *Zhou*, 1990]. Where they overlap, the one- and three-dimensional structures found in this study largely corroborate those found in earlier studies, most of which can been viewed as partial images of this complex region. For example, the shallow structures determined by *Grasso et al.* [1983], such as the relatively low velocities between Malekula and Efate, are similar to those found in this study. Between 40 and 240 km depth, the 6% gradient found by *Kaila and Krishna* [1978] is consistent with

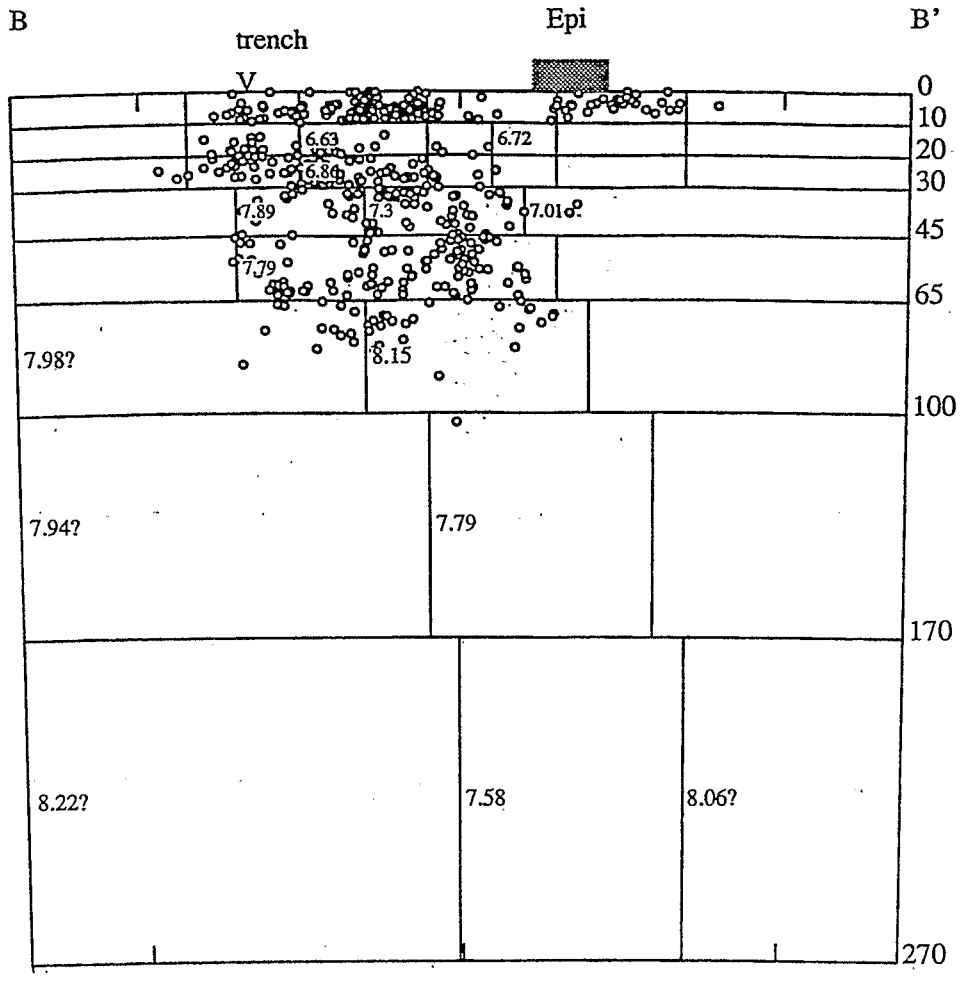

Fig. 11. Cross section along the direction B-B' as shown in Figure 2. Block velocities determined with a resolution greater than 0.85 are indicated on the figure. Velocities indicated with a question mark are considered as unreliable.

the 7% gradient of our one-dimensional structure deduced here using ISC and local data (Table 2). The deviation of the velocity in the 75-100 km depth interval in Figure 5 of *Kaila and Krishna* [1978] where velocities are significantly less than their model predicts, is consistent with the low-velocity zone found in our one-dimensional structure. *Zhou* [1990], in a study of *P* wave slab anomalies in the SW Pacific, found a cross-strike flat-lying low-velocity zone at intermediate depth in the central part of the New Hebrides islands arc (section H3 of Figure 11 of *Zhou* [1990]), although the amplitude of the anomaly is smaller (about 1%) within the area of the subducted slab and peaks at about 3% several degrees to the east of the Benioff zone.

Tectonic Inferences

Due to the fairly linear geometries of the seismic zone and of the local seismic array, most of the velocities that we consider reasonably well constrained are those within the subducted oceanic lithosphere, or at shallow depths within the overriding plate. What little information we obtained about the structure of the upper mantle is derived from the ISC data and, because of its relatively low quality, is considered less reliable.

The thickness of the crust in the upper plate appears to be around 30 km (Figure 8) where velocities jump to 8 km/s. We suggest that the velocities within the crust are governed by and reflect the interaction between the two plates. As mentioned above, the northern Santo block is a seaward protrusion of the upper plate and, in the absence of a trench, interacts directly with the DFZ. Our results show an unusually high velocity (>7.4 km/s) between 10 and 30 km beneath Santo. This high-velocity region could be an upward contortion of the Moho toward the plate boundary with an high below Santo and appears to fade southward below Malekula where these high velocities are found deeper in the fourth layer. The Moho appears to be more and more upward contorted from north Malekula to Santo. Within these high velocities, a relatively low velocity feature (Figures 5-7) originates at the surface (5.35 km/s) north of Malekula and migrates southward through layer 2 (6.18-6.59 km/s) and possibly through layer 3 (6.66-6.88 km/s). These low-velocity blocks are approximately aligned with the inferred subducted part of the southern flank of the DFZ [*Taylor et al.*, 1980].

The structure beneath the region between Malekula and Efate islands appears quite different from that beneath Santo. The high velocities found near Santo disappear to the south and are replaced by an anomalously low-velocity structure. A

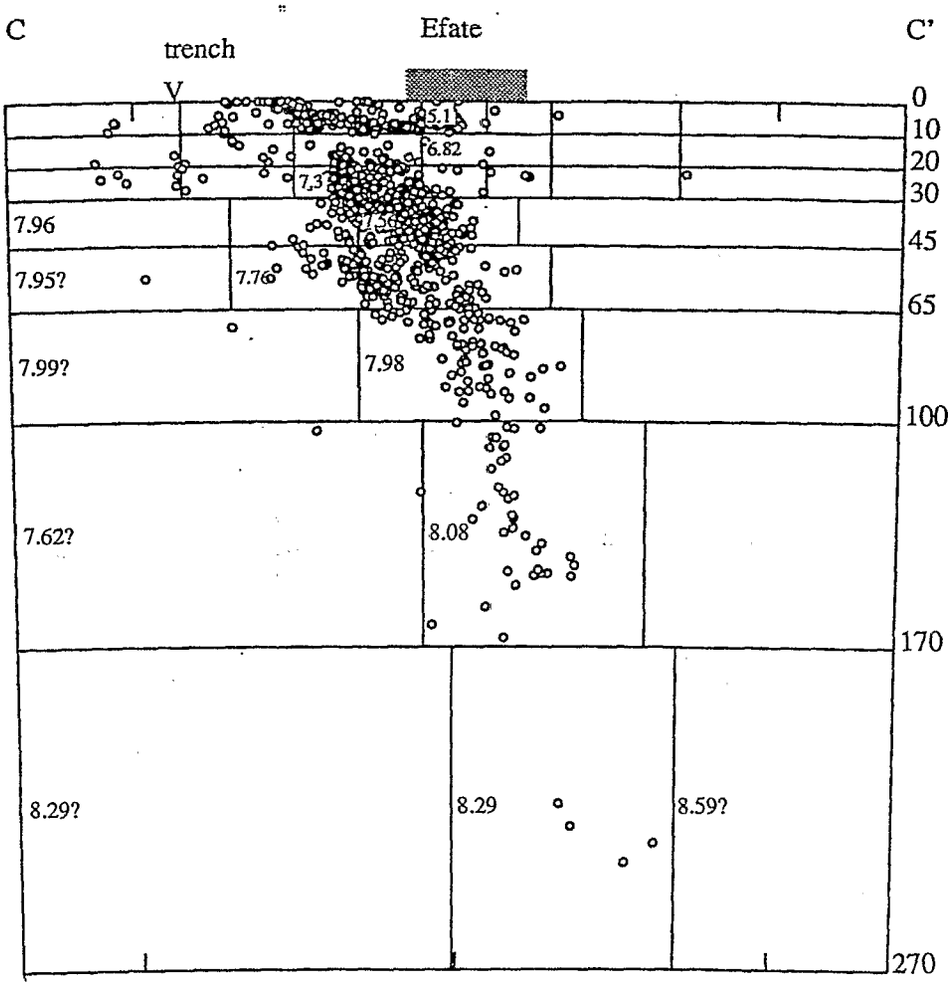

Fig. 12. Cross section along the direction C-C' as shown in Figure 2. Block velocities determined with a resolution greater than 0.85 are indicated on the figure. Velocities indicated with a question mark are considered as unreliable.

boundary between these two features appears south of Malekula where the velocity decreases from 6.8 to 6.63 km/s in layer 2 and from 6.99 to 6.86 km/s in layer 3. The southern boundary of this feature is not clearly defined, however, due to the coarse scale of the model, but a plausible candidate is the seismic boundary determined by *Chatelain et al.* [1986] which marks the northern extent of the nest of seismicity northwest of Efate.

The boundary between this low-velocity zone and a higher eastern velocity zone corresponds to the 1000-m bathymetric contour (Figure 1). The large low-velocity zone lies in a region of low level seismic activity (Figures A1and A2) as well as in the embayment in the leading edge of the upper plate. We note that *Collot and Fisher* [1989] determined two places in the New Hebrides where forearc basins are being formed by collision between seamounts and accretionary wedges: west of the northern tip of Malekula and between Malekula and Efate. These are precisely the areas where we observe anomalously low velocities, and therefore we infer that these low velocities are being caused by anomalous structure that has been subducted with the descending plate.

In contrast to Malekula, the westward protruding Efate block is associated with higher velocities trenchward in layers 2 and 3. A similar feature was noted by *Chiu et al.* [1986] and may be explained by an upward contortion of the Moho near the trench. A similar feature can been seen southward in the Erromango and Tanna regions where velocities in layer 3 are higher trenchward than beneath the islands. However, the relatively low resolution (0.40) of this structure precludes further interpretation. These observations are also in good agreement with the velocity model proposed by *Ibrahim et al.* [1980], which shows the Moho dipping from 15 km depth near the descending plate to 28 km beneath the islands.

The fourth layer (30-45 km depth; Figure 8) maps the velocity of the upper mantle and the upper part of the descending plate. We interpret those blocks with velocities around 8 km/s as belonging entirely to the upper mantle. Between Santo and Efate islands, an elongated low-velocity feature has a minimum (7.3 km/s) between Malekula and Efate islands where there is also a low of seismic activity (Figure A4). These blocks are most likely part of the descending plate. We interpret the minimum of velocity as a downward extension of the low velocity structures seen in the descending plate in the upper layers. In layer 4, however, there is an area of where velocities are much lower and extend to the back arc region (the 7.01 and 7.02 km/s velocity blocks in Figure 8). The extent of this low-velocity zone to the east and the south is unknown and then it could be either a local back arc anomaly or part of a regional anomaly beneath the North Fiji Basin.

Perhaps the most striking feature in the descending plate

revealed by this study is the large low velocity zone which overlaps the gap of seismicity (Figure 9). A study by *Marthelot et al.* [1985] showed that the extrapolated location of a subducted DFZ would coincide with this zone and that high-frequency shear waves travelling across this zone were severely attenuated. However, they could not use this observation to distinguish the existence of a thermal anomaly in the slab from a region of intense scattering. Combining their result with the velocity anomaly found in this study we infer that the subducted DFZ is associated with a positive thermal anomaly that lowers the strength of the descending plate. Assuming that the velocity contrast of about 0.3 km/s was due solely to temperature, then a velocity-temperature coefficient of $(dv_P/dt)_P = 4 \times 10^{-4}$ km/s °C [*Soga et al.*, 1966] implies a temperature difference of about 750° between the aseismic zone and the surrounding lithosphere. There is some indication that this anomalous zone extends to depths below the end of the Benioff zone (Figures 9 and 11), but these velocities are not very reliable. Because these low velocities are continuous up to layer 4 (30-45 km) the thermal effect may extend to the upper part of the Benioff zone. We note that the location of the low-velocity region coincides with a region of presently active volcanoes, notably those on Ambrym and the submarine volcanoes at the southern tip of Epi.

Acknowledgments. We thank C. Baldassari, F. Bondoux, R. Campillo, M. Chauvin (deceased) , C. Douglas, R. Foy, L. Mollard, D. Nakedau, C. Reichenfeld, J.C. Willy, E. Yakoulea, and all others involved in the data collection and analysis operations. We thank David James and an anonymous reveiwer for their thoughtful comments. This work was partially supported by USGS contract 14-08-0001-G1160 and by the Institut Français de Recherche Scientifique pour le Développement en Coopération (ORSTOM). Cornell University Institute of the Continents contribution 169.

REFERENCES

Abers, G.A., and S.W. Roecker, Deep structure of an arc-continent collision: earthquake relocation an inversion for upper mantle *P* and *S* wave velocities beneath Papua New Guinea, *J. Geophys. Res., 96*, 6379-6401, 1991.

Aki, K., and W.H.K. Lee, Determination of three-dimensional velocity anomalies under a seismic array using first *P* arrival times from local earthquakes, 1, A homogeneous model, *J. Geophys. Res., 81*, 4281-4339,1976.

Bevis, M., and B. Isacks, Leveling arrays as multicomponent tiltmeters: Slow deformation in the New Hebrides island arc, *J. Geophys. Res., 86*, 7808-7824, 1981.

Bloom, A.L., C. Jouannic, and F.W. Taylor, Preliminary radiometric ages from the uplifted Quaternary coral reefs in Efate, in Geology of Efate and Offshore Islands, edited by R.P. Ash, J.N. Carney, and A. Macfarlane, regional report, pp. 47-49, Geological Survey, Port-Vila, New Hebrides, 1978.

Carney, J.N., and A. Macfarlane, Lower to middle Miocene sediments on Maewo, New Hebrides, and their relevance to the development of the outer Melanesian arc system, *Bull. Aust. Explor. Geophys., 9*, 123-130, 1978.

Chatelain, J.L., B.L. Isacks, R.K. Cardwell, R. Prevot, and M. Bevis, Patterns of seismicity associated with asperities in the Central New Hebrides islands arc, *J. Geophys. Res., 91*, 12,497-12,519, 1986.

Chiu, J.M., B.L. Isacks and R.K. Cardwell, Studies of crustal converted waves using short-period seismograms recorded in the Vanuatu island arc, *Bull. Seismol. Soc. Am., 76*, 177-190, 1986.

Choudhury, M.A., G. Poupinet, and G. Perrier, Shear velocity from differential travel times of short period ScS-P in New Hebrides, Fiji-Tonga, and Banda Sea regions, *Bull. Seismol. Soc. Am., 65*, 1787-1796, 1975.

Chung, W.Y., and H. Kanamori, A mechanical model for plate deformation associated with aseismic ridge subduction in the New Hebrides arc, *Tectonophysics, 50*, 29-40, 1978a.

Chung, W.Y., and H. Kanamori, Subduction process of a fracture zone and aseismic ridges--The focal mechanism and source characteristics of the New Hebrides earthquake of January 19, 1969 and some related events, *Geophys. J. R. Astron. Soc., 54*, 221- 240, 1978b.

Collot, J.Y.and M.A. Fisher, Formation of forearc basins by collision between seamounts and accretionary wedges: An example from the New Hebrides subduction zone, *Geology, 17*, 930-933, 1989.

Collot, J.Y.and M.A. Fisher, The collision zone between the North D'Entrecasteaux ridge and the New Hebrides island arc, 1, Sea Beam morphology and shallow structure, *J. Geophys. Res., 96*, 4457-4478, 1991.

Coudert, E., B.L. Isacks, M. Barazangi, R. Louat, R. Cardwell, A. Chen, J. Dubois, G. Latham, and B. Pontoise, Spatial distribution and mechanisms of earthquakes in the southern New Hebrides arc from a temporary land and ocean bottom seismic network and from worldwide observations, *J. Geophys. Res., 86*, 5905-5925, 1981.

Coudert, E., R.K. Cardwell , B.L. Isacks, and J.L. Chatelain , *P*-wave velocity of the uppermost mantle and crustal thickness in the central Vanuatu islands (New Hebrides islands arc), *Bull. Seismol. Soc.Am. , 74*, 913-924, 1984.

Daniel, J., C. Jouannic, B. Larue, and J. Recy, Interpretation of the D'Entrecasteaux zone (north of New Caledonia), in *International Symposium on Geodynamics in South-West Pacific, Noumea, New Caledonia*, pp. 117-124, Technip, Paris, 1977.

Dubois, J., Contribution à l'étude structurale du S.O. Pacifique d'après les ondes sismiques observées en Nouvelle Calédonie et aux Nouvelles Hebrides, thèse de doctorat es Sciences Physiques, 160pp., Univ. de Paris, 1969.

Dubois, J., G. Pascal, M. Barazangi, B.L. Isacks, and J. Oliver, Travel times of seismic waves between the New Hebrides and Fiji Islands: A zone of low velocity beneath the Fiji Plateau, *J. Geophys. Res., 78*, 3431-3436, 1973.

Dubois, J., J. Launay, J. Recy, and J. Marshall, New Hebrides trench: Subduction rate from associated lithospheric bulge, *Can. J. Earth Sci., 14*, 250-255, 1977.

Dziewonski, A.M., and D. L. Anderson, Preliminary reference Earth model (PREM), *Phys. Earth Planet. Inter., 25*, 297-356, 1981.

Fisher, M. A., J.Y. Collot, and E. L. Geist, The collision zone between the north D'Entrecasteaux ridge and the New Hebrides island arc, 2, Structure from multichannel seismic data, *J. Geophys. Res., 96*, 4457-4478, 1991.

Gilpin, L.M., Tectonic geomorphology of Santo island, Vanuatu (New Hebrides), M.S. thesis, Cornell University, Ithaca, N.Y., 1982.

Goula, X., and G. Pascal, Structure of the upper mantle in the convex side of the New Hebrides island arc, *Geophys. J. R. Astron. Soc., 58*, 145-167, 1979.

Grasso, J.R., M. Cuer, and G. Pascal, Use of two inverse techniques: Application to a local structure in the New Hebrides islands arc, *Geophys. J.R. Astron. Soc., 75*, 437-472, 1983.

Hamburger, M.W., and B.L. Isacks, Deep earthquakes in the Southwest Pacific : A tectonic interpretation, *J. Geophys. Res., 92*, 13,841-13,854, 1987.

Ibrahim, A., B. Pontoise, G. Latham, B. Larue, T. Chen, B.L. Isacks, J. Recy, and R. Louat, Structure of the New Hebrides Arc-Trench system, *J. Geophys. Res., 85*, 253-266, 1980.

Isacks, B.L., and M. Barazangi, Geometry of Benioff zones : Lateral segmentation and downwards bending of the subducted lithosphere, in *Island Arcs, Deep Sea Trenches, and Back-Arc Basins, Maurice Ewing Ser., vol. 1*, M. Talwani and W.C. Pitman, III (editors), pp. 99-114, AGU, Washington, D.C., 1977.

Isacks, B.L., R.K. Cardwell, J.L. Chatelain, M. Barazangi, J.M. Marthelot, D. Chinn, and R. Louat, Seismicity and tectonics of the central New Hebrides island arc, *In Earthquake Prediction: An International Review, Maurice Ewing Ser., vol. 4*, edited by D. Simson and P. Richards, pp. 93-116, AGU, Washington, D.C., 1981.

Kaila, K., and V. Krishna, Upper mantle velocity structure in the New Hebrides island region, *J. Phys. Earth, 26*, S139-S153, 1978.

Karig, D., and J. Mammerickx, Tectonic framework of the New Hebrides island arc, *Mar. Geol., 12*, 187-205, 1972.

Maillet, P., M. Monzier, M. Selo, and D. Storzer, La zone D'Entrecasteaux (sud-ouest Pacifique): Nouvelle approche pétrologique et géochronologique, in Equipe de Géologie-Géophysique du Centre ORSTOM de Noumea, *Trav. Doc. ORSTOM, 147*, 441-458, 1982.

Mallick, D.I.J., and G. Neef, Geology of Pentecost, regional report, Geological Survey, 103 pp., Port-Vila, New Hebrides, 1974.

Mallick, D.I.J., and D. Greenbaum, Geology of Southern Santo, regional report, Geological Survey, 84 pp., Port-Vila, New Hebrides, 1977.

Mammerickx, J.,T.E. Chase, S.M. Smith, and I.L. Taylor, Bathymetry of the South Pacific, report, *Scripps Inst. of Oceanogr.*, La Jolla, Calif., 1973.

Marthelot, J.M., J.L. Chatelain, B.L. Isacks, R.K. Cardwell, and E. Coudert, Seismicity and attenuation in the central Vanuatu (New Hebrides) islands: A new interpretation of the effect of the D'Entrecasteaux fracture zone, *J. Geophys. Res., 90*, 8641-8650, 1985.

Mitchell, A.H.G., and J.A. Warden, Geological evolution of the New Hebrides island arc, *J. Geol. Soc. London, 127*, 501-529, 1971.

Monzier, M., J.Y. Collot, and J. Daniel, Carte bathymétrique des parties centrale et méridionales de l'arc insulaire des Nouvelles Hébrides, report, *Inst. Fr. de Rech. Sci. pour le Dév. en coop., ORSTOM*, Paris, 1984.

Pascal, G., B.L. Isacks, M. Barazangi, and J. Dubois, Precise relocation of earthquakes and seismotectonics of the New Hebrides island arc, *J. Geophys. Res., 83*, 4957-4973, 1978.

Pavlis, G.L., and J.R. Booker, The mixed discrete-continous inverse problem : Application to the simultaneous determination of earthquake hypocenters and velocity structure, *J. Geophys. Res., 85*, 4801-4810, 1980.

Pontoise, B., D. Tiffin, Seismic refraction results over the D'Entrecasteaux Zone west of the New Hebrides Arc, *Géodynamique, 1*(2), 109-120, 1986.

Roca, J.L., Essai détermination du champ de contraintes dans l'archipel des Nouvelles Hebrides, *Bull. Soc. Geol. Fr., 20*, 511-519, 1978.

Roecker, S.W., Velocity structure of the Pamir-Hindu Kush region: Possible evidence of subducted crust, *J. Geophys. Res., 87*, 945-959, 1982.

Roecker, S.W., Y.H. Yeh, and Y.B. Tsai, Three-dimensional *P* and *S* wave velocity structures beneath Taiwan: Deep structure beneath an arc-continent collision, *J. Geophys. Res., 92*, 10,547-10,570, 1987.

Roecker, S.W., J.L. Chatelain, B.L. Isacks, and R. Prevot, Anomalously deep earthquakes beneath the New Hebrides trench, *Bull. Seismol. Soc. Am., 78*, 1984-2207, 1988.

Soga, N., E. Schreiber, and O.L. Anderson, Estimation of bulk modulus and sound velocities of oxides at very high tempetratures, *J. Geophys. Res., 71*, 5315-5320, 1966.

Tarantola, A., and B. Valette, Inverse problem = Quest for information, *J. Geophys., 50*, 159-170, 1982.

Taylor, F.W., B.L. Isacks, C. Jouannic, A.L. Bloom, and J. Dubois, Coseismic and Quaternary vertical movements, Santo and Malekula islands, New Hebrides Islands Arc, *J. Geophys. Res., 85*, 5367-5381, 1980.

Thurber, C., and W. Ellsworth, rapid solution of ray tracing problems in heterogeneous medias, *Bull. Seismol. Soc. Am., 70*, 1137-1148, 1980.

Zhou, H.-W., Mapping of *P*-wave slab anomalies beneath the Tonga, Kermadec and New Hebrides arcs, *Phys. Earth Planet. Inter., 61*, 199-229, 1990.

J.L. Chatelain, Institut Français de Recherche Scientifique pour le Développement en Coopération, ORSTOM, Noumea, New Caledonia.

B.L. Isacks and R. Prevot, Institute for the Study of the Continents, Cornell University, Ithaca, New York.

S.W. Roecker, Department of Earth and Environmental Sciences, Rensselaer Polytechnic Institute, Troy, New York .

(Received April 22, 1991;
revised July 5, 1991;
accepted July 5, 1991.)